

INTEGRATION OF CORE AND DOWNHOLE ACOUSTIC MEASUREMENTS
- SHEAR AND COMPRESSIONAL

John A. Nieto and David P. Yale*

Mobil North Sea Limited

* Mobil Research and Development Corporation

Abstract The acquisition of reliable formation shear and compressional velocity data (V_s and V_p , respectively) is becoming increasingly important^s for better calculation of rock properties for use in both geophysical and petrophysical applications.

A study has been made using core samples from the Rotliegendes sandstones of the southern North Sea in order to evaluate better the laboratory measurement of both shear and compressional velocities and to improve the application of downhole velocity measurement. Excellent correlations between the log and core velocities were found.

Transforms have been established for the Rotliegendes formation to relate compaction-corrected core porosity to shear velocity, as a basis for predicting porosity from downhole shear velocity measurements. The downhole shear velocity measurements were provided by the Mobil dipole-sourced Shear Wave Acoustic Log (SWAL) which gave reliable shear velocity measurements even in cased hole. The downhole compressional velocities were acquired with the monopole-sourced Mobil Long Spaced Acoustic Log (LSAL).

Results of the laboratory measurements indicate that core velocities are sensitive to overburden stress and fairly insensitive to sample size.

Comparisons have been made of V_p/V_s ratio from core and log data, which is the input parameter^p for many of the petrophysical and geophysical applications. Poisson's ratios calculated from acoustic velocities ("dynamic") compare well with those measured directly during triaxial testing ("static").

INTRODUCTION

Compressional acoustic ('sonic') well logging tools have been used for many years, primarily to determine the porosity of reservoir rock formations. The ability to record entire waveforms has introduced another sonic application, namely calculation of mechanical properties of the formation via shear wave velocity extraction. The calculation of the ratio of compressional and shear velocities, the base parameter for most mechanical properties work has been facilitated recently by the introduction of dipole shear acoustic logging tools, such as Mobil's SWAL (Shear Wave Acoustic Log) tool and most recently Schlumberger's DSI tool. The dipole shear wave acoustic logging tools allow a more robust determination of formation shear velocity than "full waveform" monopole logging tools, even in cased hole (Medlin and Alhilali 1990).

An understanding of the mechanical properties of the reservoir has long been important in well stimulation and sand control. With certain assumptions, the Poisson's ratio of the formation, which can be derived from the ratio of compressional and shear velocities, can be used to determine in-situ stress within the reservoir, which controls fracturing pressure. Young's modulus is an important parameter in fracture modelling, and Bulk modulus (with its related property, pore compressibility) is important for reservoir engineering analysis. Shear modulus and shear strength are important parameters for understanding sand control.

Another important application for reliable acoustic compressional and shear velocity measurements is to enhance seismic interpretation, and to give a better understanding of whether AVO anomalies are caused by lithology contrast or by hydrocarbons.

This paper presents the results of a study made to assess the value of integrating core shear and compressional velocity measurements with the most robust downhole compressional and shear velocity measurements acquired with the new generation of acoustic logging tools.

Laboratory shear and compressional velocity data from two different laboratories, using both plugs and whole cores, have been integrated with downhole acoustic velocity data acquired with the Mobil LSAL (Long Spaced Acoustic Log) and SWAL dipole shear logging tool. The study was made upon cores from the Rotliegendes sandstone formation in the Southern Gas basin of the U.K. North Sea. The two wells chosen for the study were drilled vertically and were

completely water bearing to eliminate any possible hydrocarbon correction to the downhole acoustic logs. The study area is shown together with a generalised stratigraphic column in Figure 1.

A comparison has been made between log and core acoustic velocities and mechanical properties, with transforms derived to aid in the determination of porosity in this area.

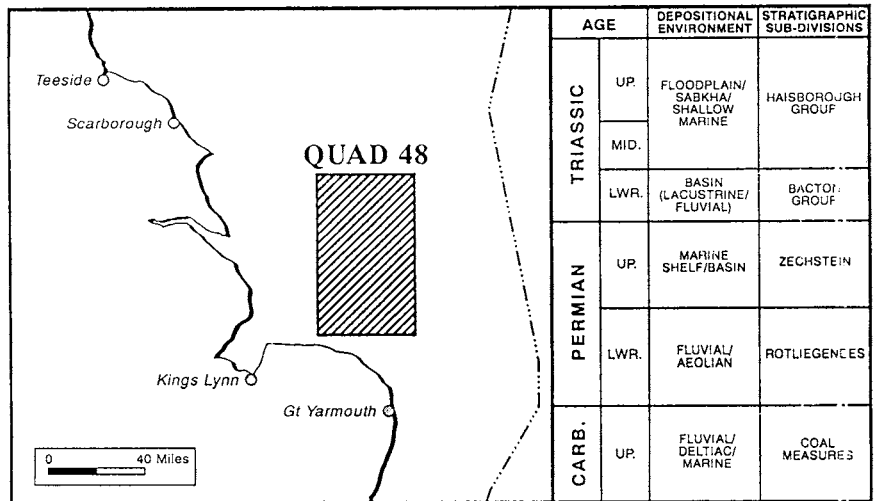


FIGURE 1 The study area location with generalised stratigraphy

LABORATORY MEASUREMENT TECHNIQUES

Sample Preparation

Both the wells used for the study were comprehensively cored, and a selection of core material was available to evaluate sensitivity of acoustic velocity to sample size. Six samples measured from well 'A' were 4" diameter by 3-4" long whole cores, seven samples measured on well 'B' were 2 7/8" diameter and 3-4" long whole cores. Further, 1 1/2" and 1" plug samples were taken from well 'B'. A list of sample details is shown in Table 2, which is to be found later in the "Results" section. All plug samples were cut vertically to the core axis to facilitate comparison with downhole acoustic logs. Plug samples were cut using

Dual, damped, broadband P and S acoustic transducers are located in a high pressure, titanium housing, at each end of the core sample. Titanium is used for these housings because of the similarity between acoustic impedance of titanium and "rock", which provides better energy transmission (acoustic coupling) than either, say, aluminium or stainless steel.

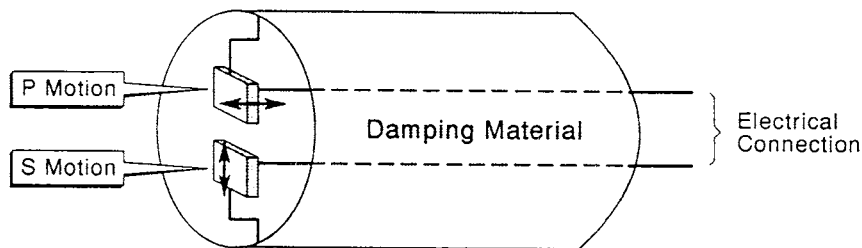
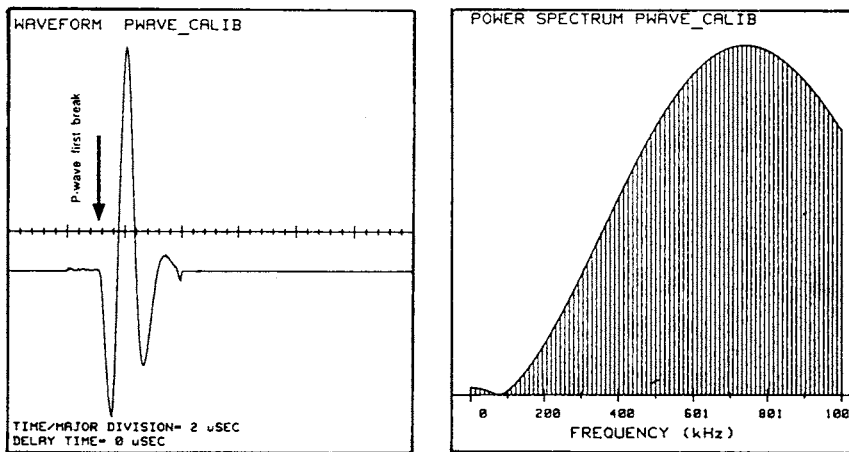


FIGURE 3 Schematic diagram of transducers

The transducers themselves are piezoelectric crystals specifically oriented within the housing to transmit and receive preferentially either P or S mode acoustic energy. Figure 3 illustrates the concept schematically. The transducers are driven by a DC voltage spike of 200-600 volts which lasts 500 nanoseconds. The received acoustic signal is amplified 20 to 60 dB using the acoustic pulser/receiver unit shown in Figure 2. The entire acoustic system is controlled by a mini-computer which regulates confining and pore pressure, records waveforms at specified pressures, switches between P and S wave transducers, and calculates acoustic velocity and power spectrum from a user defined first break time.

Method. The brine saturated core samples are placed into the pressure housing as shown in Figure 2. A positive pore pressure of 1000 psi was maintained throughout the testing to ensure complete brine saturation of the core sample. Confining stress was increased gradually by the computer control, and acoustic measurements made continually up to 5000 psi, equivalent to the 'reservoir effective total stress' of 4000 psi (Nieto, Yale and Evans, 1990).

The system is calibrated by measuring the first break time of both P and S waves through the titanium transducer housings, as determined by the operator. This travel time is then subtracted from the travel times of all other measurements. Figure 4a illustrates the time domain waveform of the transducer housings for the P wave. Figure 4b shows the power spectrum or energy versus frequency of the calibration waveform. The frequency axis shown is from 0 Hz to 1000 kHz which facilitates comparison with the other illustrations in the text. The travel time is measured on a digital oscilloscope and corrected by the computer, which subtracts the transducer calibration travel time to give a corrected core sample travel time. The acoustic velocity is then determined by dividing sample length by this corrected travel time, for both P and S modes.



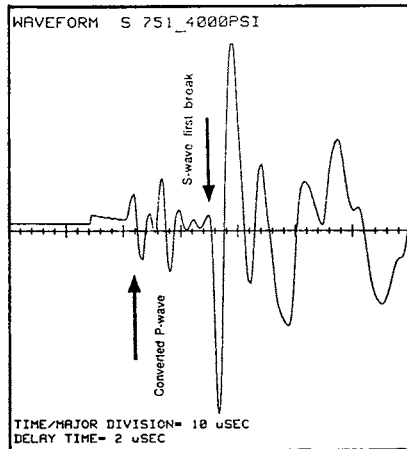
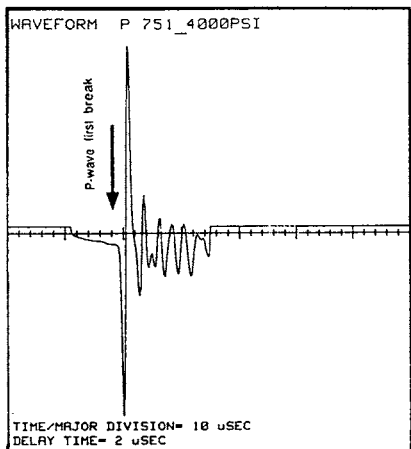
(a)

(b)

**FIGURE 4 System calibration: (a) P-waveform
(b) P-wave power spectrum**

Figure 5 shows recorded P and S waveforms for sample X751 from well B at 4000 psi total effective stress. The first breaks are distinct, facilitates operator picking for subsequent travel time determination. Figure 5b shows some mode-converted P-wave energy which arrives ahead of the S-wave energy. Travel times through the core sample for

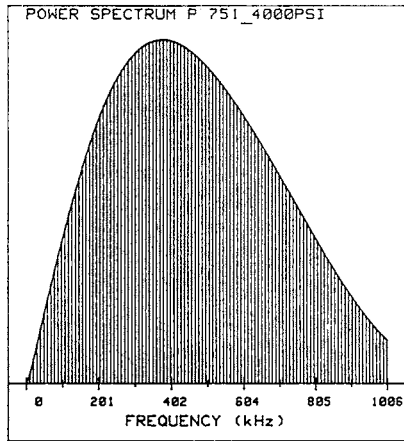
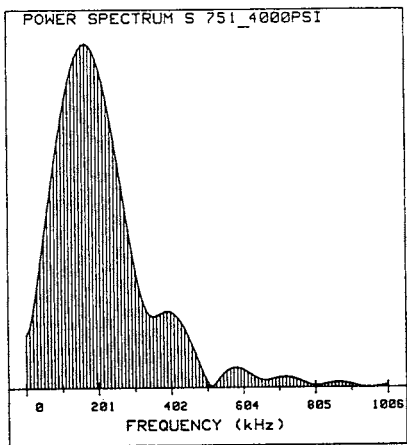
this P-wave and that in Figure 5a are identical after compensating for slight travel time differences through the transducer housings.



(a)

(b)

FIGURE 5 Waveforms, sample X751 at 4000 psi (a) P-wave (b) S-wave



(a)

(b)

FIGURE 6 Power spectra, sample X751 at 4000 psi: (a) P-wave (b) S-wave

Figure 6 shows the corresponding power spectra of the P and S waves. These spectra show the 'filtering' effect of reservoir rock, which absorbs the higher frequency energy. The frequency of the measured P wave ranges from 300 kHz to 800 kHz, and of the S wave from 200 kHz to 500 kHz. The power spectra illustrated are normalised to the peak energy of a particular spectrum, to allow for the varying attenuation between modes. The S-wave signal for example is about 10-15 dB lower in strength than the P-wave signal, which is in turn 20-40 dB lower than the calibration waveform signal.

Porosity

Ambient (zero net stress) porosity measurements were made on all samples. Reservoir condition porosities were determined by measuring brine expulsion from the sample under increasing hydrostatic confining pressure in conjunction with acoustic velocity measurements. The reservoir total effective stress was taken to be 4000 psi as discussed in the acoustic velocity section. The compaction correction to convert ambient core porosities to reservoir-condition porosities was then determined. A correction factor of 0.94 of ambient porosity was appropriate for all samples.

Pore Compressibility

Pore compressibilities were calculated from the above porosity reduction data by differentiating the volume of brine expelled with respect to applied stress, and then dividing the result by the pore volume, at each pressure. Figure 7 illustrates the result.

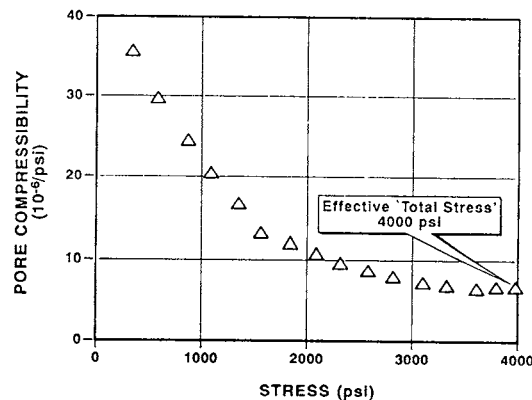


FIGURE 7 Rotliegendes Sandstone - Compressibility Test

Static Mechanical Properties

Static mechanical properties were measured triaxially by a third laboratory on unsaturated plug samples, $1\frac{1}{2}$ " diameter by 2" long, at 4000 psi confining stress. The apparatus consists of a pressure vessel with rams extending from either end to allow the application of axial stress independently of confining stress. Inside the pressure vessel, the sample deformation during testing is measured by Linear Variable Differential Transducer. An axial LVDT measures deformation in the sample length, and 3 radial LVDT's measure sample deformation in the horizontal plane as axial load is applied.

Mechanical properties were determined over the first 5000 psi of axial loading above the confining stress. Static mechanical properties are detailed in Table 1. Load, axial and radial deformation are recorded, and the slopes of these lines are used to compute Young's modulus and Poisson's ratio.

THEORY OF MECHANICAL PROPERTIES MEASUREMENTS

Mechanical properties can be measured in the laboratory during triaxial tests (referred to as "static" tests), or they can be approximated from measurements of compressional and shear acoustic velocities and rock bulk density ("dynamic" measurements). The equations which relate acoustic velocities to mechanical properties are based upon elasticity theory (Jaeger and Cook, 1976) and make the assumption that the material is purely elastic. In practice, no reservoir rock material is purely elastic; indeed, many exhibit marked inelasticity. This is one of the main reasons for the often observed discrepancy between "static" and "dynamic" mechanical properties. A further reason for differences is the frequency and loading conditions at which the measurements are made. "Dynamic" mechanical properties are derived from elastic loading of a volume of rock at rates between 1 000 and 1 000 000 cycles per second, the acoustic wave frequencies, with deformations due to the loading in the order of 10^{-8} to 10^{-6} strain (length change over length of body or material affected by the load). Conversely, "static" mechanical properties are measured at rates of 10^{-2} to 10^{-4} cycles per second (minutes up to hours per loading cycle), and with deformations of 10^{-4} to 10^{-2} strain.

In the reservoir, rock deformation rates are even slower than static tests. Static measurements are much more

indicative than dynamic measurements of the mechanical properties of the reservoir which control the stress and deformation of the reservoir. It is therefore very important that acoustic logs, which measure mechanical properties dynamically, can be translated into the more representative static values.

Static Mechanical Properties

A summary of the principal static mechanical properties is given below.

Pore compressibility

Pore compressibility is calculated from the equation:-

$$C_p = (\Delta PV/PV) / \Delta P$$

where P is reservoir stress.
PV is pore volume

Young's Modulus and Poisson's Ratio

Young's modulus is defined as:

$$E = (\Delta L/L) / \Delta \sigma$$

where L = sample length (axially)
 ΔL = change in sample length
 $\Delta \sigma$ = change in axial stress during uniaxial loading

Poisson's ratio is defined as:

$$\nu = (\Delta r/r) / (\Delta L/L)$$

where Δr = sample radius change during a uniaxial loading.

Δr , ΔL and $\Delta \sigma$ are determined from plots made during triaxial tests where the confining pressure is held constant and the axial load is increased.

Bulk Modulus

Bulk modulus is calculated from Poisson's ratio and Young's modulus assuming purely elastic solids using:

$$K = E / [3(1 - 2\nu)]$$

Dynamic Mechanical Properties

As an acoustic wave passes through a sample of rock, the wavelength and frequency of the disturbance is such that the pore fluid cannot move from pore to pore as the pore space is deformed by the elastic wave. The pore fluid therefore "supports" some of the elastic loading due to the wave's passage. Compressional velocities are higher in water saturated rock than in those with some free gas since water is incompressible and gas is not. Since the "frequency" of static tests and the "frequency" of stress changes in the reservoir (even during fracturing tests) are orders of magnitude lower, the pore fluid can move from one region to another and does not support any of the elastic load.

Calculation of dynamic mechanical properties, directly from raw acoustic velocities on fully water saturated rocks, results in higher moduli and Poisson's ratios, because one is measuring a rock/water composite in contrast with static test which just measure the properties of the rock frame (referred to as "undrained" case). Biot-Gassmann theory (Gassmann 1951; Biot 1956; Geertsma and Smit; 1961) allows us to take out the water contribution to compare better the static values with the dynamic values (referred to as "drained" case).

The equation which relates the "drained" dynamic bulk modulus, K_d (often referred to as the "frame" modulus), to the "undrained" or water-saturated dynamic bulk modulus is:

$$K_d = (K_s Q - 1) / (Q + K_s / K_o^2 - 2 / K_o) \quad \text{after Biot-Gassmann}$$

$$\text{where } Q = (1 / K_o + \phi / K_w - \phi / K_o)$$

$$K_w = 1 / C_w \quad (\text{water compressibility})$$

$$K_o = \text{bulk modulus of matrix } (1 / C_g)$$

$$C_g = \text{matrix compressibility}$$

$$K_s = \text{bulk modulus from water saturated velocities}$$

and

$$K_s = \rho (V_p^2 - 4/3 V_s^2)$$

where V_p and V_s are the compressional and shear acoustic velocities of a water saturated core.

TABLE 1 Summary of formulae and symbols used for dynamic and static

$$\begin{aligned}
 E &= 9K\mu/(3K + \mu) \\
 K &= \rho(V_p^2 - 4/3 V_s^2) \\
 K &= E/3(1 - 2\nu) \\
 C_p &= [1/K - (1 - \phi)C_g]/\phi \\
 \mu &= \rho(V_s^2) \\
 \mu &= E/(2 + 2\nu) \\
 \nu &= (3K - 2\mu)/2(3K + \mu) \\
 \nu &= [(V_p/V_s)^2 - 2]/2[(V_p/V_s)^2 - 1] \\
 \nu &= (E/2\mu) - 1
 \end{aligned}$$

E = Young's modulus
 ν = Poisson's ratio
 μ = Shear modulus
 K = Bulk modulus
 C_p = Pore compressibility
 V_p = Compressional velocity
 V_s = Shear velocity
 ρ = Bulk density
 ϕ = Porosity

Note: If V_p , V_s are in decimeters/second and $\rho = \text{g/cc}$, the K and μ will be in bars.

The shear modulus is not affected by the pore fluid (since the pore fluid cannot support any shear loading) so that:

$$\mu = \rho V_s^2$$

The other dynamic moduli (Young's modulus, Poisson's ratio) can be calculated using elasticity theory from K and μ (see Table 1 for a summary of all the elasticity relations used in this paper).

With one exception, all the dynamic moduli and Poisson's ratios in this paper have been calculated from the "drained" dynamic bulk modulus and dynamic shear modulus. The exception is the "undrained" Poisson's ratio, which is calculated from the acoustic velocities of fully water saturated core samples.

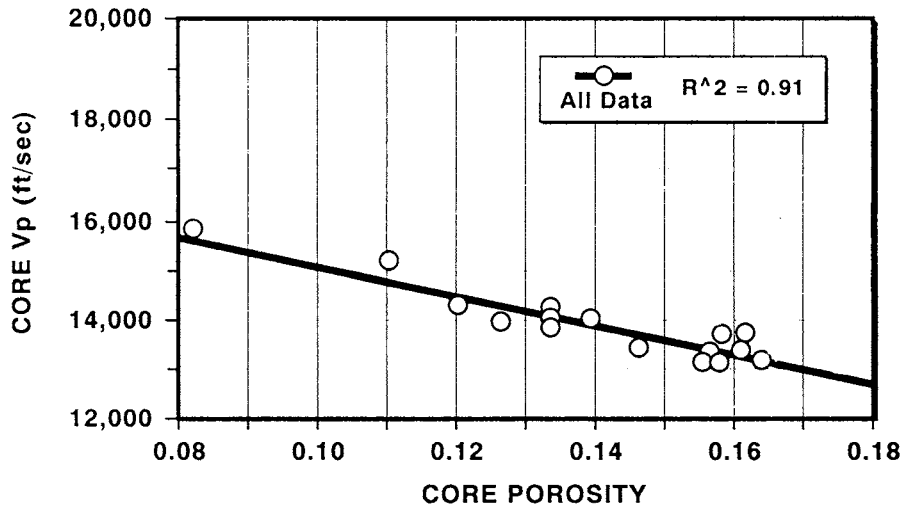


Figure 8 Core acoustic compressional velocity vs compaction corrected core porosity

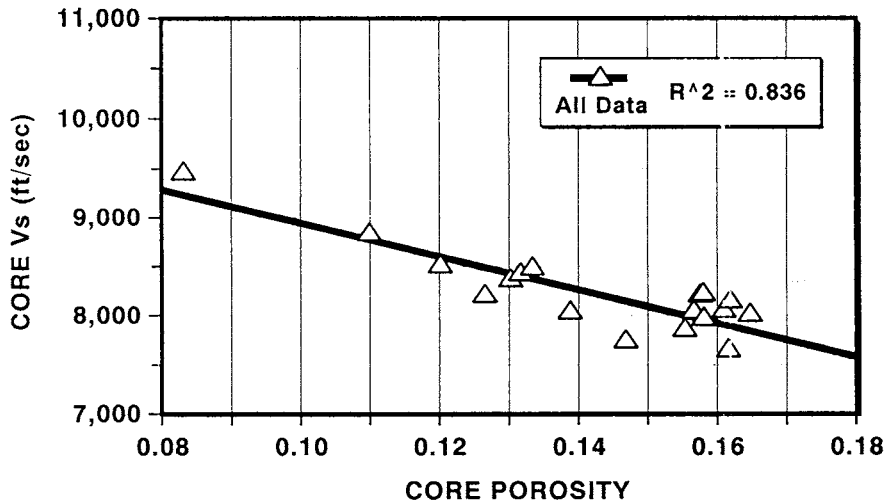


Figure 9 Core acoustic shear velocity vs compaction corrected core porosity

for compressional travel times. The shear travel times were similarly good, 123.0 $\mu\text{sec}/\text{ft}$ for core against 124.5 $\mu\text{sec}/\text{ft}$ for log travel times, a difference of 1.2%.

Conversely, core acoustic velocity data in well B were dispersed discretely throughout the logged interval. Figure 11 again indicates excellent agreement between log and core data.

This agreement lends credence to the laboratory methods used and confidence in the derived porosity - velocity transforms (equations 1 and 2). Application of these transforms over the whole well gives a very good agreement between core porosities and those derived from compressional-wave, shear-wave and density measurements. This agreement is shown in track 5 of Figures 10 and 11. The 'shear porosity' algorithm may well prove useful in hydrocarbon bearing Rotliegendes, and also in cased hole in other neighbouring wells.

Effect of Stress and Sample Size on Acoustic Velocity

Acoustic velocity is routinely measured at simulated in-situ stress conditions because of the large dependence of acoustic velocity on stress (Wyllie et al, 1956; Domenico, 1977; Han et al., 1986). Acoustic velocities were measured at a simulated in-situ stress of 4000 psi for all the samples, but many were also measured at 0 psi and 1000 psi. These data showed that for P-waves the 2000 psi velocity is on average 5% lower than the 4000 psi pressure and the 1000 psi value is 15% lower. The ambient or 0 psi velocity is on average 35% lower. For S-waves the difference is even more striking. The 2000 psi value is 7.5% lower and the ambient measurement is more than 50% lower than the 4000 psi value. This difference in the stress dependence of shear and compressional waves has been noted before (Han et al., 1986) and manifests itself as a decrease in Poisson's ratio with increasing stress. Figures 10 and 11 show core velocities measured at 2000 psi and 4000 psi compared to wireline log data, and illustrate clearly this marked dependence of core velocity data on confining stress. The importance of calculating the correct reservoir total effective stress is also apparent from these data.

The data in Table 2 were measured on samples ranging from 1" diam to 4" diam. Both V_p and V_s plotted against core porosity or wireline log velocity show no apparent effect of sample size. However, the study has indicated that larger samples (>2" diam and >2" long) are preferable for several reasons.

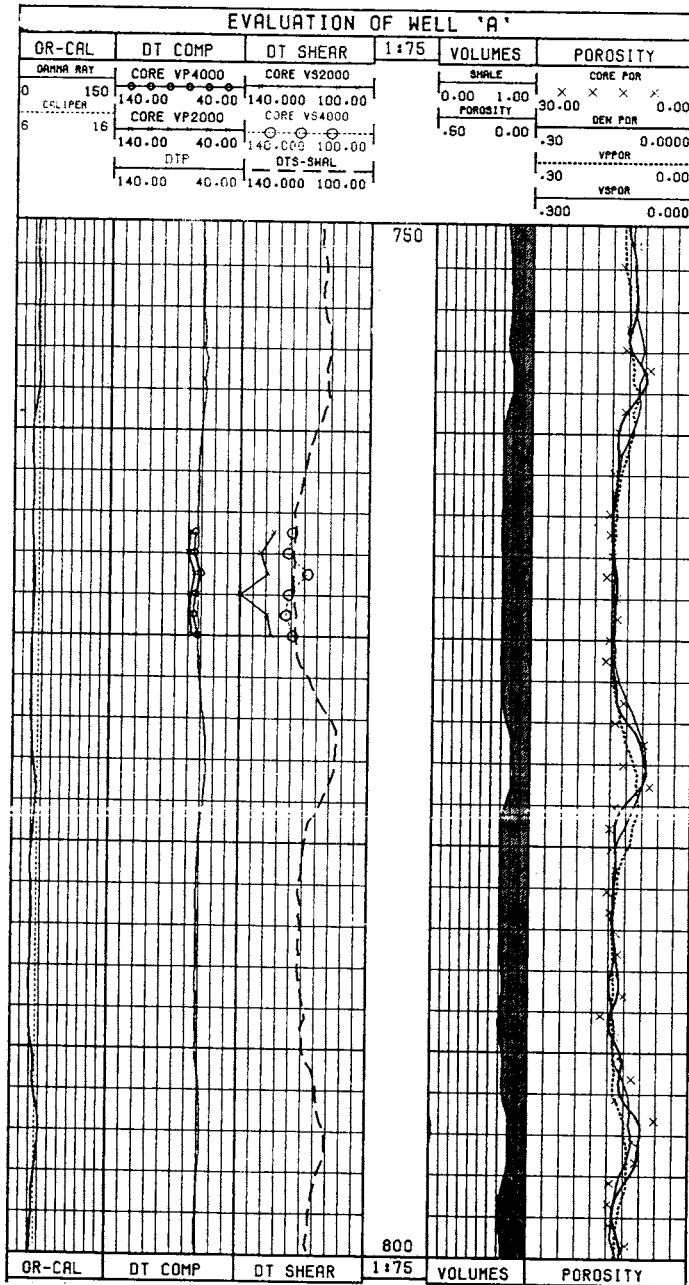


Figure 10 Computer processed interpretation Well A

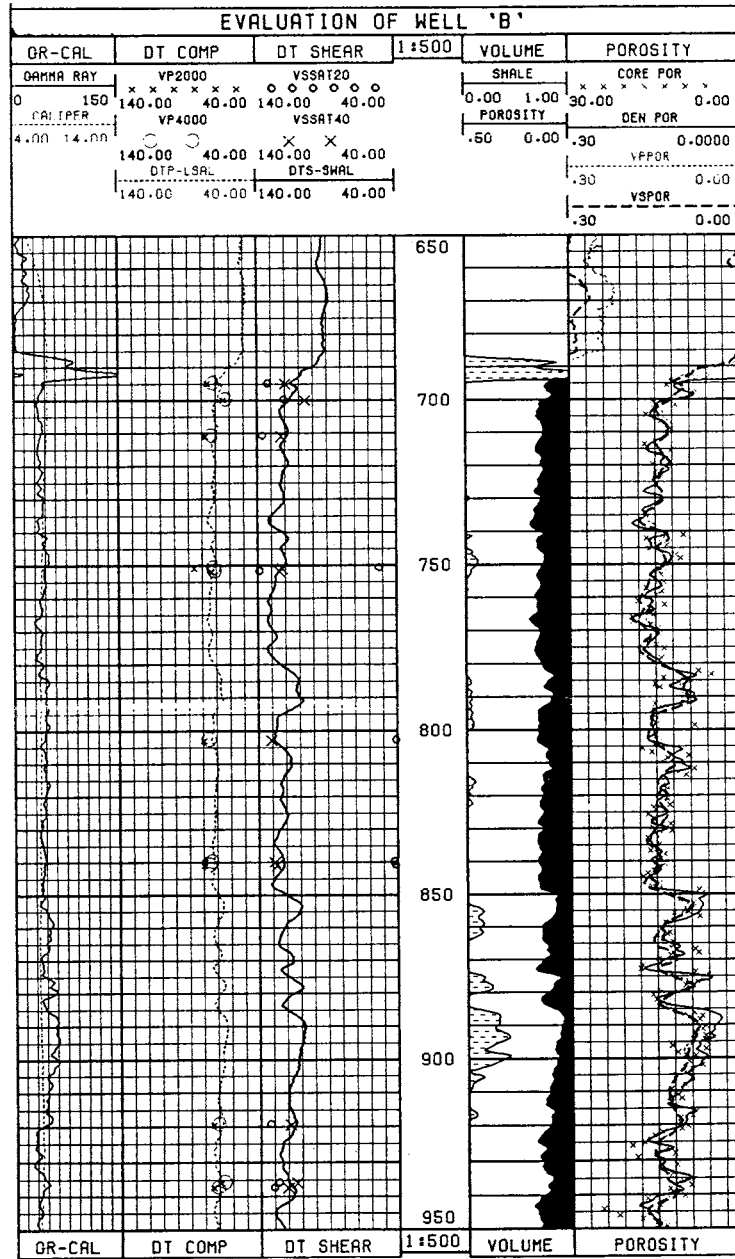


Figure 11 Computer processed interpretation Well B

- 1) Larger sample diameters prevent reflections from the sample sides which can degrade signal quality.
- 2) Larger formation volumes give a better representation of formation properties, and may therefore facilitate integration with wireline logs.
- 3) Longer samples allow lower frequency energy to be used while still maintaining body wave propagation. Velocity dispersion due to grain scattering (Winkler and Plona, 1982) is generally not evident below 800 kHz.

Pore Compressibilities

Figure 7 shows pore compressibility as a function of effective stress for one of the core samples. The compressibility at 4000 psi stress corresponds well with the compressibility measured during the triaxial tests on other samples. These compressibility data show that porosity at 4000 psi is approximately 0.94 of the porosity at ambient (zero effective stress) conditions, an observation which is in line with the value used elsewhere in this area.

Mechanical Properties

Figure 12 makes a comparison of the "static" and "dynamic" (drained) Poisson's ratios. There is a fairly good correlation, especially considering that there is such a small range of Poisson's ratios represented by the data (for reservoir rocks, Poisson's ratio varies between 0.05 and 0.45). Table 2 shows the poor correlation between "dynamic (undrained)" and "static" Poisson's ratio. Because the pore fluid effect only contributes to compressional velocity, it increases the "dynamic" (undrained) Poisson's ratio to unrealistically high values. Since Poisson's ratio from logs is used frequently to estimate in-situ stresses, these data show the importance of correcting for the pore fluid in the acoustic velocity measurements before calculating Poisson's ratio.

Figures 12, 13 and 14 show the poor correlation between the "static" and "dynamic" for other mechanical properties (pore compressibility, Young's modulus). For Young's moduli the "dynamic" values are 3 to 5 times higher than the static values (since compressibility is the reciprocal of modulus, "static" pore compressibilities are 2 to 4 times higher than "dynamic" pore compressibilities). Some authors claim (Montmayeur and Graves, 1985) that much of the difference between "static" and "dynamic" moduli is due to the fact that undrained dynamic moduli are used rather than drained

dynamic moduli. But, as can be seen here, even the drained dynamic moduli are significantly higher than the static moduli. Only with rocks which have high modulus and low porosity do the static and dynamic moduli approach one another (Jaeger and Cook, 1976; Walls, 1987).

This suggests that for many reservoir rocks, correlations between "static" and "dynamic" (drained) moduli must first be computed for various rock types before the well logs can be used with any confidence to derive the mechanical properties. Poisson's ratio appears to be the exception to this rule. This is because Poisson's ratio is the ratio of Young's modulus and shear modulus and consequently this compensates for any systematic differences in these measurements (see Table 1).

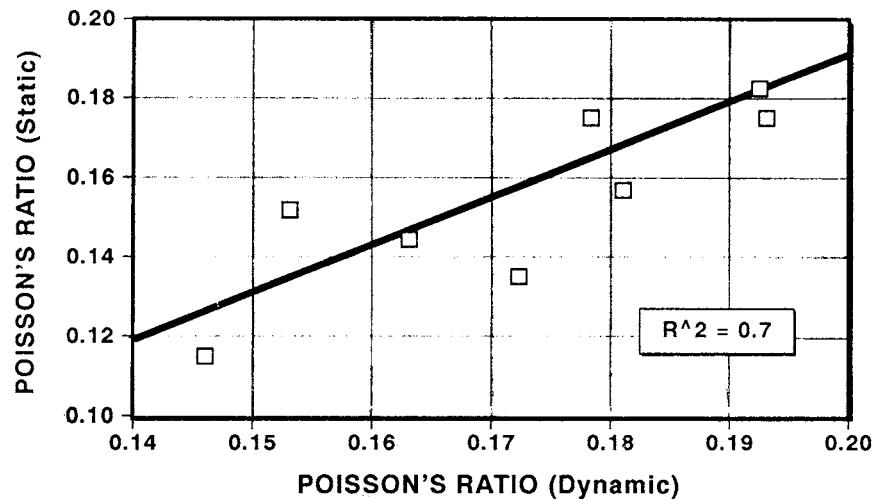


Figure 12 Poisson's ratio "dynamic vs static"

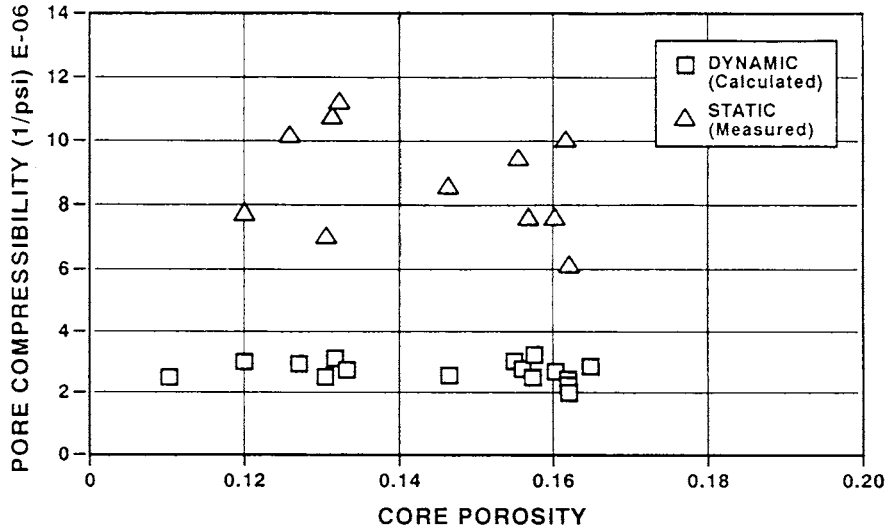


Figure 13 Pore compressibility "dynamic vs static"

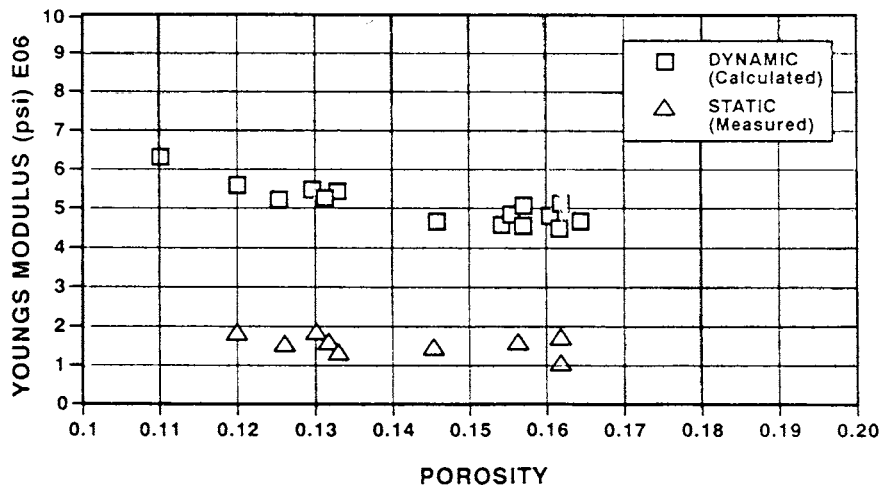


Figure 14 Youngs modulus "dynamic vs static"

CONCLUSIONS

- 1) There is a good correlation between core acoustic velocities and well log acoustic velocities for the studied well intervals.
- 2) Porosity/velocity transforms are more robust for compressional velocity than shear velocity in the porosity interval studied, but both shear and compressional velocity correlate well with porosity. Further, application of the transforms in both wells shows good agreement between compressional, shear density and core porosity over the whole Rotliegende.
- 3) "Dynamic" (drained) Poisson's ratios correlate well with "static" Poisson's ratios, suggesting that Poisson's ratios can be determined from the well logs, with the appropriate correction.
- 4) Acoustic velocities must first be corrected for the pore fluid using the Biot-Gassmann relationship before calculating "dynamic" (drained) moduli.
- 5) "Dynamic" (drained) Young's, bulk, and shear moduli do not correlate well with their "statically" measured counterparts. We suggest that well logs not be used to derive these parameters unless extensive correlations from core are first developed.
- 6) Acoustic compressional and shear velocity measurements are very sensitive to confining stress especially at lower confining stresses.
- 7) Sample size:- though core acoustic velocity measurements appear to be insensitive to sample size, we find larger samples i.e. 2" to 4" diameter, 2" to 6" long are preferable.

ACKNOWLEDGEMENTS

The authors wish to thank the management of Mobil North Sea Limited for their permission to publish this study. Thanks are also due to R.D. Moore of Mobil Research and Development Corporation and R. Harting of Core Laboratories, Dallas for detailed laboratory work, and A. Humble and Z. Booth for their help in preparation of this paper.

REFERENCES

- BIOT, M.A. (1956) Theory of propagation of elastic waves in a fluid-saturated porous solid. "J. Acoust. Soc. Am.", Vol. 28, p. 168-178.

- DOMENICO, S.M. (1977) Elastic properties of unconsolidated porous sand reservoirs, "Geophysics", Vol. 42, p. 1339-1368.
- GASSMANN, F. (1951) Über die elastizität poröser medien, "Vierteljahrsschrift der Naturforschenden Gesellschaft in Zürich", Vol. 96, p. 1-23.
- GEERTSMA, J. and SMIT, D.C. (1961) Some aspects of elastic wave propagation in fluid-saturated porous solids, "Geophysics", Vol. 26, p. 169-181.
- HAN, D., NUR, A. and MORGAN, D. (1986) Effects of porosity and clay content on acoustic properties of sandstones and unconsolidated sediments, "Geophysics", Vol. 51, p. 2093-2107.
- JAEGER, J.C. and COOK, N.G.W. (1976) Fundamentals of rock mechanics. "London : Chapman and Hall".
- MEDLIN, W.L. and ALHILALI, K.A. (1990) Shear wave porosity logging in sands, "SPE paper #20558" 65th Annual SPE.
- MONTMAYEUR, H. and GRAVES, R.M. (1985) Prediction of Static elastic/mechanical properties of consolidated and unconsolidated sands from acoustic measurements, "Society of Petroleum Engineers", paper #14159, 60th Annual SPE.
- NIETO, J.A., YALE, D.P. and EVANS, R.J., (1990) Core compaction correction - a different approach. "Advances in Core Evaluation", EUROCAS1. Gordon and Breach.
- WALLS, J.D. (1987) Poisson's ratio and mechanical properties from core and well log measurements, "Society of Petroleum Engineers" paper #16795, 62nd Annual SPE.
- WINKLER, K.W. and PLONA, T.J. (1982) Technique for measuring ultrasonic velocity and attenuation spectra in rocks under pressure, "Jour. Geophys. Res.", Vol. 87, p.10, 776-10, 780.
- WYLLIE, M.R.J., GREGORY, A.R. and GARDNER, L.W. (1956) Elastic wave velocities in heterogeneous and porous media, "Geophysics", Vol. 21, p.41-70.

